Environ Monit Assess (2023) 195:108
https://doi.org/10.1007/s10661-022-10735-z

Spatio-temporal variation of nitrate based on Landsat 8 in Playa Colorada bay, Sinaloa, Mexico

Luis Carlos González-Márquez · Franklin M. Torres-Bejarano · Ivette Renée Hansen-Rodríguez · Ramiro Ahumada-Cervantes

Received: 17 January 2022 / Accepted: 5 November 2022

Abstract Characterizing water quality in coastal waters through spatial observations is challenging, due to spatial and temporal variations in water composition. Nitrate, an important compound for water quality assessment, has received little attention in estimates made from satellite measurements, even though it can be estimated using models generated from multispectral images. Since nitrate is a non-optically active parameter that can be correlated with optically active parameters, it was related to bands of the visible and infrared spectrum, captured in Landsat-8 images, and used to generate empirical models to estimate the spatio-temporal variation of nitrate concentration in the Playa Colorada Bay, in the state of Sinaloa Northwest Mexico. Four sampling campaigns were performed, two in spring and two in fall. Nitrate nitrogen (NO_3-N) concentration ranged between 0.69 and 1.80 mg/L, values higher than those recommended in the Mexican ecological criteria of water quality for the protection of marine aquatic life in coastal areas. Generated models showed a significant relationship ($P < 0.05$) between NO_3-N and band reflectance in the infrared (band 5) and short-wave infrared (band 6 and band 7) spectra of Landsat-8 imagery. The B6 band appeared in all models selected to estimate NO_3-N in the bay. These results evidence the potential of Landsat-8 images for the estimation of nitrate in the coastal waters of Sinaloa, México.

Keyword Coastal zone monitoring · Water pollution · Remote sensing · Empirical models

Introduction

Nutrient excess in water may cause negative effects in aquatic systems, such as excessive growth of plants and algae, dissolved oxygen depletion or exhaustion, biogeochemical cycle disruption, and biodiversity loss (Haggard et al., 2005; Hutchinson, 1973; Smith et al., 1999). In the ocean, nitrogen is regarded as the limiting nutrient, whereas estuaries are considered transition zones concerning nitrogen and phosphorus (Caponze & Hutchins, 2013; Correll, 1998). Nitrogen, mainly nitrates and ammonia, has been associated with algal blooms on the coasts of North Sinaloa, Mexico (Martínez-López et al., 2008). The Playa Colorada bay is part of the Playa Colorada-Santa María La Reforma coastal lagoon system, an

L. C. González-Márquez (✉) · I. R. Hansen-Rodríguez · R. Ahumada-Cervantes
Engineering and Technology Department, Universidad Autónoma de Occidente, Unidad Regional Guasave, Sinaloa, México
e-mail: luis.gonzalez@uadeo.mx

L. C. González-Márquez · R. Ahumada-Cervantes
Doctorado en Sustentabilidad, Universidad Autónoma de Occidente, Unidad Regional Guasave, Sinaloa, México

F. M. Torres-Bejarano
Environmental Engineering Department, Universidad de Córdoba, Montería, Colombia

Published online: 14 November 2022

essential ecosystem for populations of blue shrimp (*Litopenaeus stylirostris*) inhabiting the Pacific Ocean waters of Mexico, as well as other animal and plant species of ecological and commercial concern (Lyle-Fritch, 2003). Located in the north-central part of the Sinaloa, the bay provides water for the shrimp farms established along its margins. The bay receives aquaculture and municipal wastewaters, as well as agricultural wastewaters from Irrigation Districts (ID) 063 and 074 (González-Márquez et al., 2014). Little is known about the pollution load caused by these activities, and how this load may affect environmental health. Monitoring parameters related to water quality can be essential for bay management, allowing to identify and forecast related environmental problems (Kouadri et al., 2022a, b; Mishra et al., 2021). In Mexico, monitoring is performed through the national water quality monitoring network, seeking to know the spatiotemporal trends of physical, chemical, and biological parameters in surface and groundwater (Comisión Nacional del Agua, 2022). The information generated, however, is not readily accessible at a single observation level, but only as annual averages or as categorical classifications of water quality. In the Playa Colorada bay, there is only one monitoring station, where evaluations of total nitrogen, nitrates, total phosphorus, phosphates, total suspended solids, chemical oxygen demand, biological oxygen demand, etc. are made. An average of four measurements are made per year, providing insufficient information for making spatial and temporal evaluations, as well as for defining management strategies (Mishra et al., 2022). The NO_3-N concentration recommended in the Mexican Ecological Criteria of Water Quality for the protection of marine aquatic life in coastal areas is 0.04 mg/L (Diario Oficial de la Federación, 1989).

Satellite remote sensing is a feasible tool for generating information on water quality over large areas, solving the problems posed by conventional methods (Lim & Choi, 2015; Wang & Yang, 2019). Estimates of water quality parameters are based on the relationship between apparent optical properties, as captured by satellite sensors, and the inherent optical properties of water (Mouw et al., 2015). The resulting information can be used to generate empirical models by correlating water quality parameters, evaluated both in situ and in the lab, with reflectance value captures in satellite images (González-Márquez et al., 2018; Guo et al., 2021; Lim & Choi, 2015; Torbick et al., 2013; Wu et al., 2010). These models usually show reliable results when applied to the same sites where they were generated (Chang et al., 2014). Empirical models to estimate nutrient concentration in water are not common due to the lack of a signal that can be detected by satellite sensors (Goes et al., 2004). Despite that, there are models able to detect nutrient concentration, as it can be correlated to optically active water components (Goes et al., 1999). Nitrogen and phosphorus do not have a direct impact on the visible spectrum of the water body, but they do affect color indirectly because they promote algae growth (Dong et al., 2020). In estuaries, nitrogen concentration can be related to the concentration of suspended solids, an optically active compound (Paudel et al., 2019). Nutrients can be released to the water column through biological recycling of organic compounds, as well as from suspended particles and resuspended particles in estuaries with changing salinities (Bruesewitz et al., 2017; Tappin et al., 2010). Nitrate can be estimated when related to optically active compounds (Goes et al., 1999; Topp et al., 2020). In freshwater, nitrate can be associated with chromophoric dissolved organic matter and nitrogen oxidation by aerobic bacteria (Khattab & Merkel, 2013) and in oceans with sea surface temperature and chlorophyll-a (Chen & Chen, 2003). Few studies have been done focusing on generating models to estimate non-optically active parameters in water from satellite measurements (Amanollahi et al., 2017; Guo et al., 2021; Khattab & Merkel, 2013), and only one study has generated models for estimating nitrates in coastal waters (Wang et al., 2018). However, non-optically active parameters are also an important part of water quality assessment because even though their estimation through multispectral imaging is challenging, the generation of empirical models can contribute to complementing the missing information in space and time.

In this study, visible and infrared spectra reflectance bands, captured with the Operational Land Imager (OLI) sensor aboard Landsat-8, are correlated to nitrate concentration in the waters of the Playa Colorada bay, to generate empirical models and estimate their spatial variation. Although the limitations of empirical models for estimating nutrients through multispectral images are well known, these models can be used to complement the information generated through conventional methods; they can be used to estimate nutrient concentrations in areas within the same water bodies studied, where originally no in situ parameters were evaluated or any samples were collected for laboratory analysis.

Materials and methods

Study area

Playa Colorada bay, located in Sinaloa, Northwest Mexico (25º 13′ 30″ N; -108º 21′ 30″ W), has tropical dry weather, with a rainy season ranging from June to October with an average precipitation of 468.8 mm. The period of highest precipitation is from July to September. The average annual temperature, maximum temperature and minimum temperature are 24.1, 45.5, and − 6 ºC, respectively. The average annual evaporation is 2391 mm (Climate Computing project, 2016; Lyle-Fritch, 2003). The bay has an area of 6000 ha and is part of the Laguna Playa Colorada-Santa María La Reforma coastal lagoon system. The length and width of the bay are 15.5 km and 10.5 km, respectively; approximately 517 pixels long and 350 pixels wide from a Landsat image. It has been a Ramsar site since February 2, 2004 (Ramsar, 2022). The most important use of the bay is fishing for shrimp, mullet, crab, and clams, as well as other scale fish (Lyle-Fritch, 2003). Shrimp farming and irrigation agriculture are important economic activities in the basin. Although most drainages discharging into the bay area have an agricultural origin; untreated municipal wastewaters and shrimp farm wastewaters are also discharged into these drainages (Fig. 1). Playa Colorada Bay is the main source of water for the shrimp farms located in the eastern and western municipalities of Guasave and Angostura, respectively.

Sampling and water analysis

Four sampling campaigns were carried out in the bay, two in spring (May 27, 2015 and June 14, 2016) and two in fall (December 12, 2014 and December 5, 2015). Between six and fourteen sampling sites were characterized in each campaign (Table 1). Sampling sites were distributed all over the bay water surface (Fig. 1). A Van Dorn bottle (La Motte, model JT-1) was used to take 0.5 L samples from the first 40 cm of the water column. 100 ml of water were filtered through 0.45 µm nylon membranes (Millipore, HNWP) and stored in plastic containers. Before each sampling event the containers were washed and rinsed with a 1:1 hydrochloric acid solution (analytic grade), then rinsed again with MilliQ® water (MilliQ-Plus; resistivity > 18 MΩ cm). Samples were stored on ice and transported to laboratory. Nitrate nitrogen (NO_3-N) was assessed in the filtered samples

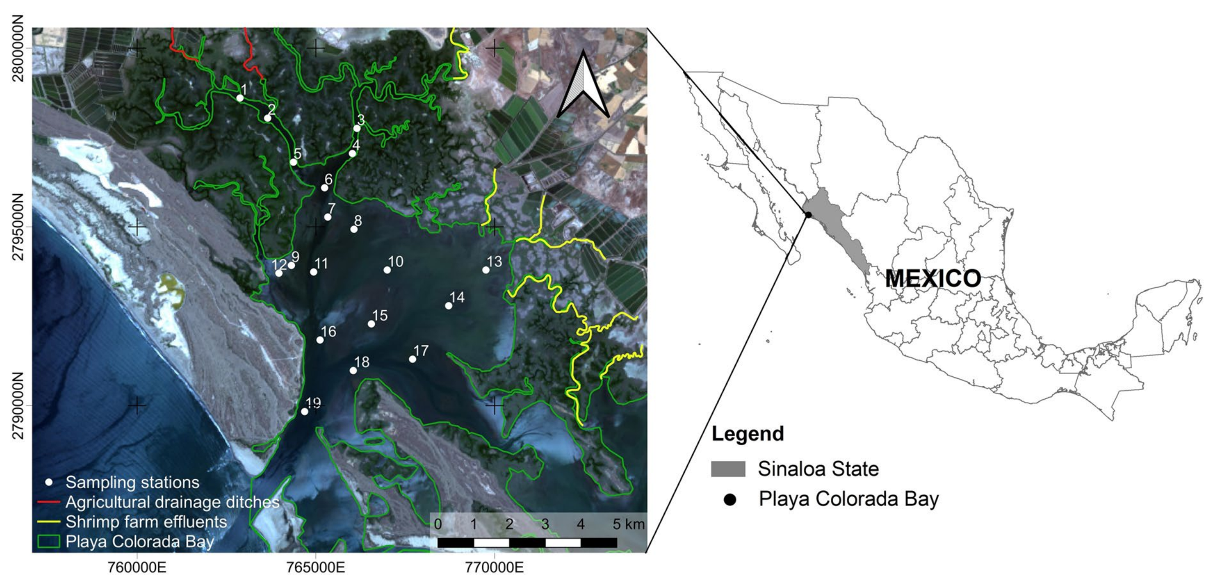

Fig. 1 Location of the study area and sampling sites in Playa Colorada Bay

Table 1 NO_3-N concentrations in Playa Colorada bay

Sampling site	December 2014 NO_3–N (mg/L)	May 2015 NO_3–N (mg/L)	December 2015 NO_3–N (mg/L)	June 2016 NO_3–N (mg/L)
1	ND	ND	0.90	1.00
2	ND	0.95	0.80	1.10
3	ND	ND	1.30	1.80
4	ND	1.30	1.30	1.20
5	ND	1.10	1.10	1.55
6	1.00	1.10	1.30	1.70
7	ND	ND	0.90	1.50
8	ND	0.93	ND	ND
9	ND	ND	0.80	1.70
10	0.90	1.00	ND	ND
11	0.70	1.00	1.50	ND
12	ND	1.00	ND	ND
13	0.80	0.90	ND	ND
14	ND	1.25	1.60	1.80
15	ND	0.85	1.00	1.60
16	1.00	0.80	1.20	ND
17	1.00	0.69	1.50	ND
18	ND	ND	1.20	1.30
19	ND	1.30	ND	ND
Min	0.70	0.69	0.80	1.00
Max	1.00	1.30	1.60	1.80
Average	0.90	1.01	1.17	1.48
Standard deviation	0.126	0.183	0.264	0.284
N	6	14	14	11

ND no data, *N* number of data

by the cadmium reduction method (Hach method 8039), 24 h after the samples were taken. A VIS spectrophotometer (Hach DR3900) was used for NO_3-N determination. Duplicate measurements were taken for quality control.

Image acquisition and processing

All samplings, except those taken in 2014, were planned to coincide with the days in which Landsat-8 took images of the study area, in agreement with previous recommendations for water quality parameter estimation. (Kloiber et al., 2002). Three Level-2 images from Landsat-8 (path 33; row 42), with atmospheric correction, were acquired from the U. S. Geological Survey (https://earthexplorer.usgs.gov); surface reflectance images, generated from the Land Surface Reflectance Code (LaSRC) (Vermote et al., 2016). The RGB image of the study area was generated in QGIS (version 3.12), reflectance values were extracted and nitrate distribution maps were generated in the bay. Only seven of the 11 bands generated by Landsat-8, with a spatial resolution of 30 m, were used to generate the models. The bands used were band B1 (coastal/aerosol; 0.43–0.45 µm), band B2 (blue; 0.450–0.51 µm), band B3 (green; 0.53–0.59 µm), band B4 (red; 0.64–0.67 µm), band B5 (near-infrared; 0.85–0.88 µm), band B6 (shortwave infrared 1; 1.57–1.65 µm), and band B7 (shortwave infrared 2; 2.11–2.29 µm).

Statistical analysis

Prior to model determination, a Shapiro–Wilk test was performed to determine whether the data (reflectance values and nitrate concentrations) was normally distributed. When the data did not show a normal distribution, it was normalized using a decimal logarithm. Models were generated through Stepwise linear regression using Matlab 2015, with NO_3-N as the dependent variable; single band reflectance and band-combinations (band ratio and band multiplication), extracted from Landsat-8 images, were used as independent variables. Three scenarios were considered for the generation of the models. In scenario one, the results of the May, June, and December (spring and fall) samplings were considered; in scenario two, only the results of May and June (spring) were considered. In scenario three, models were generated for each of the carried out samplings. In scenarios one and two, seventy percent of the data was used to generate the models and 30% to validate them (Fig. 2). The coefficient of determination (r^2) and the root mean square error (RMSE) were applied to assess the performance of each model.

Results and discussion

An overview of the measured nitrate concentrations in Playa Colorada Bay is presented. The generated models from Landsat-8 images and the validation processes are described in detail. The spatial distribution of NO_3-N is then presented in maps.

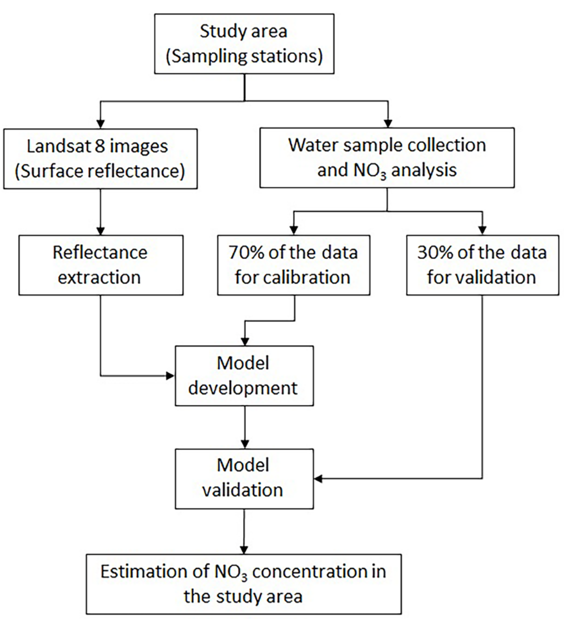

Fig. 2 Framework for predicting NO_3-N concentration from Landsat-8 imagery

Nitrate concentration in Playa Colorada bay

The average concentration of NO_3-N, considering the results of the four sampling campaigns, was 1.16 mg/L, with a standard deviation of 0.30 mg/L. The maximum obtained value, recorded in June of 2016 at sampling sites 13 and 14, was 1.80 mg/L. The minimum value, recorded at sampling site 17 in May of 2015, was 0.69 mg/L. Observed NO_3-N concentrations were always higher than 0.04 mg/L, the level recommended in the Mexican Ecological Criteria of Water Quality for the protection of marine aquatic life in coastal areas (DOF, 1989). Average NO_3-N concentrations in the bay showed an increasing trend over time, with the lowest concentrations occurring in December 2014 and the highest in June 2016 (Table 1).

Model generation and validation

Through linear stepwise regression analysis, satisfactory models were generated revealing a significant relationship between NO_3-N concentrations evaluated in the bay and reflectance values ($P<0.05$) from Landsat-8 images. The models with a lower number of variables, higher r^2 and lower RMSE were selected to estimate NO_3-N in the bay (Table 2). The comparison between measured and estimated NO_3-N concentrations is shown in Fig. 3 (scenario two) and Fig. 4 (scenario three). The model generated in scenario one presented the lowest r^2 and the highest RMSE of the three scenarios. The likely reason for the poor accuracy of the regression model for scenario one could have been the large spectral variability of the water, because that scenario used nitrate concentrations obtained in two seasons of the year (spring and fall). The changing nature of the components of coastal and inland waters is one of the main disadvantages of empirical models (Chang et al., 2014).

In scenario two, the simplest model only included the B6 band (short-wave infrared 1). Despite the relatively low r^2 value (r^2=0.657) for this model (Fig. 3a), the difference between measured and estimated concentrations was low, with an RMSE of 0.202 mg/L (Fig. 3b). The model with the highest r^2 was obtained with data from December 2016 (r^2=0.824), corresponding to scenario three (Fig. 4); however, May presented a low r^2 and for June no statistically significant models could be generated (Table 2).

Table 2 Models to estimate NO_3-N

Scenario	Models*	Month	RMSE	r^2
1	NO_3-N = 1.0534 + 16.871 * B6	May, December, and June	0.256	0.275
2	**NO_3-N = 2.5116 + 0.57621*Log B6**	May and June	0.202	0.657
3	NO_3-N = 1.9792—0.60992 * (B5/B7) + 0.083417 * (B5/B7)^2	May	0.146	0.517
	NO_3-N = -482.29 + 358.48 * Log B5 - 615.43 * Log B6 + 68,901 * B7 + 122.98 * (Log B5 * Log B6) – 34,682 * (Log B5 * B7) + 54,005 * (Log B6 * B7) - 153.27 * (Log B6)^2	December	0.163	0.824

Models in bold were selected to estimate NO_3-N in the bay. For June, no statistically significant models could be generated

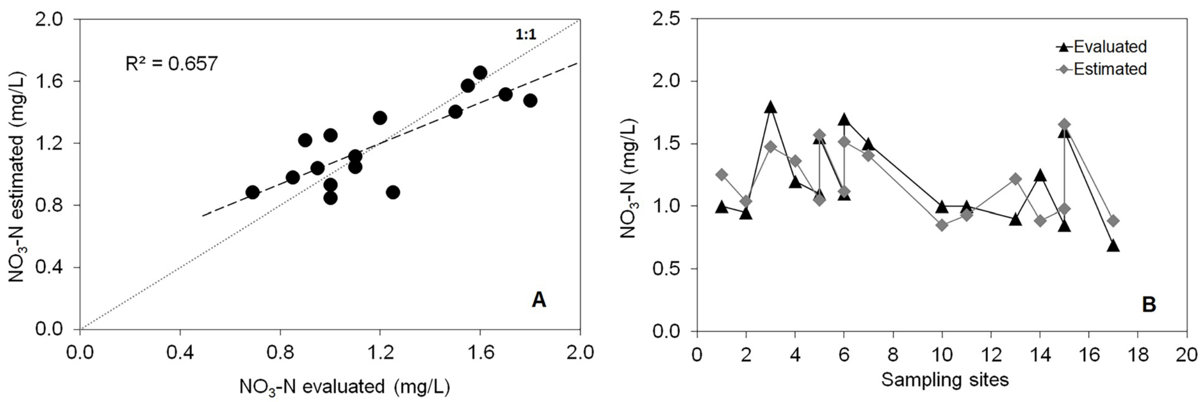

Fig. 3 The relationship between measured and estimated NO_3-N with the model generated from scenario two and Landsat-8 images. **A** Gray and black dashed lines are the line 1:1 and the regression line, respectively; **B** NO_3-N evaluated and estimated at sampling sites

Considering that similar atmospheric conditions and water composition can occur in the bay in spring, the model from scenario two (Generated using 70% of the May and June nitrate concentrations) was validated with NO_3-N concentrations that were not considered in the model generation (30% of the nitrate concentrations); the relationship between measured and estimated concentrations showed an r^2

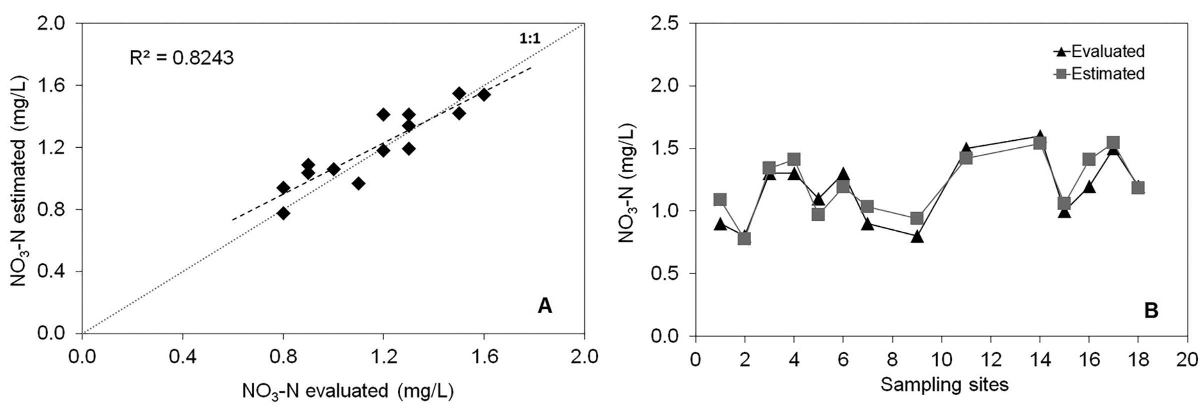

Fig. 4 The relationship between measured and estimated NO_3-N with the model generated from scenario three (December data) and Landsat-8 images. **A** Gray and black dashed lines are the line 1:1 and the regression line, respectively; **B** NO_3-N evaluated and estimated at sampling sites

like that of the model generation (r^2=0.659) (Fig. 5). In June 2016, the average reflectance of bands B1 to B7, at the location of the sampling stations, was almost two times higher than that of May 2015, with a greater difference between near infrared and short-wave infrared than among the bands of the visible spectrum (Fig. 6). The difference in reflectance values could be due to the variation in the concentration of suspended solids in the bay water. The increase in suspended solids favors the increase in reflectance, mainly in the red and infrared bands.

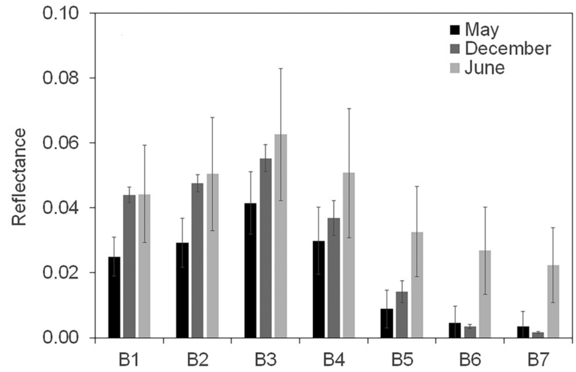

Fig. 6 Changes in the average reflectance captured by Landsat-8 OLI in Playa Colorada bay, during May 27 and December 5, 2015 and June 14, 2016

Spatial distribution of NO_3-N

The application of empirical models to satellite images allowed generating distribution maps of NO_3-N concentrations for all the bay surface, in May and December 2015, and June 2016 (Fig. 7). Distribution patterns of NO_3-N concentration were different in the three months. In general terms, the lowest concentrations were found in May and the highest in June. In May, the highest NO_3-N concentrations occurred mainly along the shores of the bay (Fig. 7a); in June were found in the eastern part of the bay (Fig. 7c). In December, the highest concentrations were found in the southern part of the bay (Fig. 7b). There is significant aquaculture development within the basin of the Playa Colorada bay, with shrimp production starting in May and ending in late November; as well as two important irrigation districts in which two agricultural cycles take place, starting in November and ending in June, maize being the main crop in the region. Due to these activities, the bay is constantly receiving elevated nitrate concentrations throughout the year. These factors may be influencing the concentrations present in the bay to be higher than those recommended by the ecological criteria for water quality (DOF, 1989).

In May and June water channels, connecting shrimp farms with the north and northeast part of the bay can be observed (Fig. 7a, c, respectively). Unlike the influents that discharge into the bay from the north, shrimp farm wastewaters that enter from the northeast do not cross mangrove areas. Mangrove wetlands can significantly reduce nitrogen and phosphorus in shrimp pond wastewater (Wang et al., 2021). The effect of such discharges can be seen in

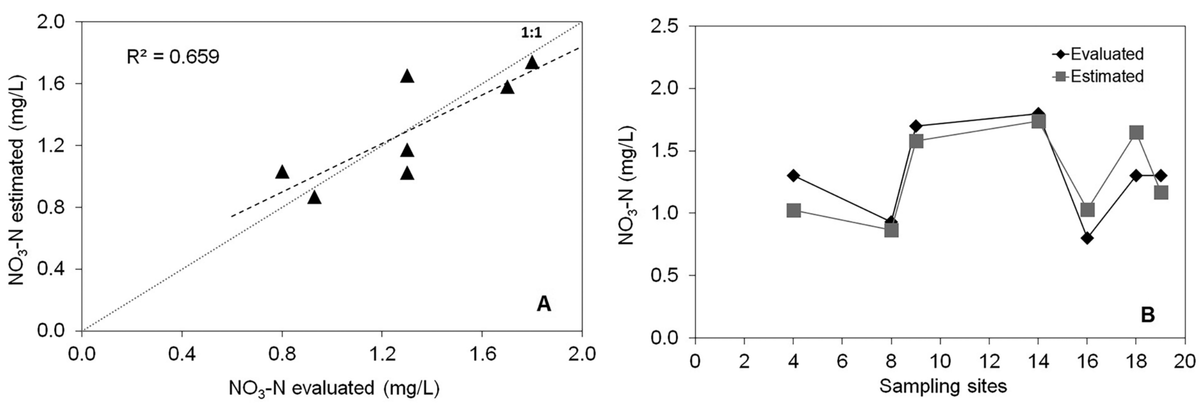

Fig. 5 Validation of the generated NO_3-N model with scenario two data (May 2015 and June 2016 data). **A** Gray and black dashed lines are the line 1:1 and the regression line, respectively; **B** NO_3-N evaluated and estimated at sampling sites

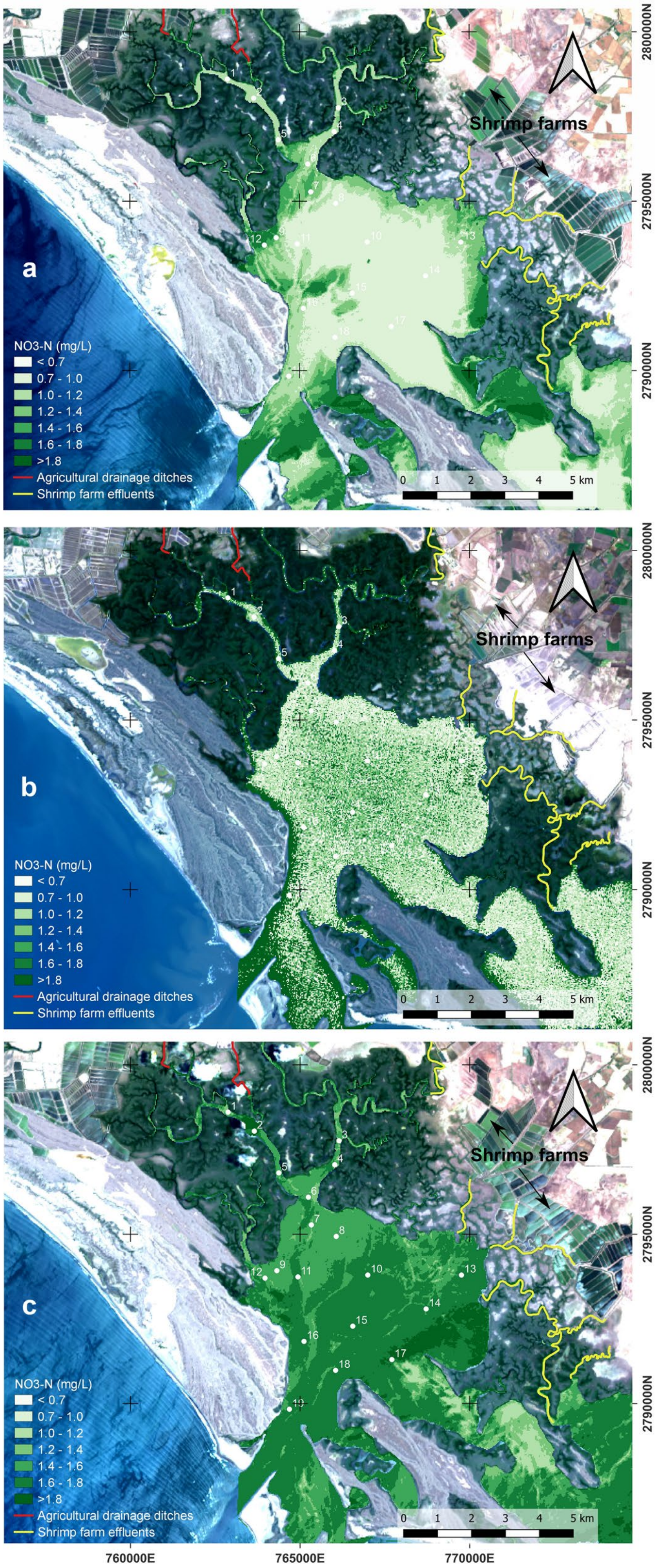

Fig. 7 Spatial distribution of estimated NO_3-N concentrations in Playa Colorada bay; **a** May 2015; **b** December 2015; **c** June 2016

Fig. 7a, mainly on the bay shores where the highest concentrations of nitrates occur. The first shrimp harvest begins in May and lasts approximately three months, which means that during this period the amount of wastewater that enters the bay from shrimp farms increases; the effect of this activity is shown in Fig. 7c, where compared to May, a higher concentration of nitrates is observed in the whole bay water. In December, the main source of wastewater is from agricultural activities, which favors a more homogeneous distribution of nitrate throughout the bay (Fig. 7b). Because shrimp farms are not operating during December, high nitrate concentrations are not observed on the northern and eastern shores of the bay.

Ruiz-Fernández and Páez-Osuna (2004) reported maximum NO_3-N concentrations of 1.8 mg/L from shrimp pond effluents in southern Sinaloa, consistent with the values obtained in this study in June 2016. Results that show the negative influence of shrimp farm wastewater discharge in the bay by increasing nitrate concentration. Nitrate has been associated with algal blooms on the coasts of northern Sinaloa (Martínez-López et al., 2008); therefore, the contribution of nitrates, through the discharge of wastewater from shrimp farms into the bay, may be having negative consequences for the ecosystems as well as for shrimp farming, considering that Playa Colorada Bay is its main source of water. NO_3-N measurements made on the northern coast of Sinaloa between November 1999 and August 2000 revealed concentrations 30 times lower than those obtained in this study (Martínez-López et al., 2008). These concentrations differ from those in this study, as they were taken in sampling sites located on the shoreline, outside the bays and coastal lagoons in the zone.

In the ocean, nitrate estimation methods from space relate the reflectance of satellite images with sea surface temperature and chlorophyll-a; these parameters are strongly correlated to phytoplankton growth (Chen & Chen, 2003), and nitrate concentration is estimated from both of them (Goes et al., 1999; Joo et al., 2018). Khattab and Merkel (2013) satisfactorily estimated nitrate concentrations of freshwater bodies with empirical models, finding a B2 (0.52–0.60 μm)/B3 (0.63–0.69 μm) relationship with Landsat-5 in summer, as well as with thermal bands of Landsat-7 images in spring. In a freshwater wetland, Amanollahi et al. (2017) studied the relationship between nitrate and spectral band reflectance of Landsat-8 bands, through linear regression analysis and neuronal networks; however, the resulting models generated low r^2 values (<0.28). Masocha et al. (2018) estimated nitrate concentrations at a reservoir in subtropical Africa, using Landsat-8 images; this study identified the B6/B5 relationship as a promising combination for nitrate estimations in the reservoir (r^2=0.53). In coastal waters, Wang et al. (2018) found a significant correlation (r^2=0.68) between nitrate concentrations measured in the East China Sea and the red band (660 nm) of the Geostationary Ocean Color Imager (GOCI). The models generated in the present study differ from those obtained in the mentioned studies above; however, it agrees with those reported by Barrett and Frazier (2016) regarding the importance of the B6 band for estimating the concentration of water constituents. Barrett and Frazier (2016) found that reflectance in the B6 band was significantly correlated with both chlorophyll and turbidity, as a result of the relationship between B6 band reflection and algae/plant production for the case of chlorophyll, as well as its relationship with suspended sediments, chlorophyll and other dissolved organic matter for the case of turbidity. The relationship between the B6 band and nitrate concentration found in this research could be caused by the indirect relationship between nitrate and bay water components, such as algae and suspended sediments. Nitrate concentration plays an important role in algal growth.

Conclusions

Empirical models were generated to estimate water nitrate concentration in the Playa Colorada Bay. These models showed a significant relationship between nitrate and bands reflectance of the infrared spectra of Landsat-8 (P<0.05). Nitrate, an important compound for water quality assessment, has not received much attention in estimates made from satellite measurements, even though it can be estimated using models generated from multispectral images. Our results show the potential of Landsat-8 images, in particular the infrared spectrum bands, in the generation of empirical models to estimate nitrate concentrations in Playa Colorada Bay.

The application of the models could help to understand the spatial and temporal distribution of nitrates, as well as to locate and evaluate the influence of municipal, agricultural and aquaculture wastewater discharges in the bay. Considering that Playa Colorada bay is the main source of water for aquaculture farms located in the east and west of the municipalities of Guasave and Angostura, respectively, those who manage such farms may also benefit from the use of the models generated in this research. Any future research related to the effect of excess nutrients on the environmental health of the bay, could benefit from the use of this data; as can the users of the results that are generated by the National Water Quality Measurement Network with an increase in the available information related to the concentration of nitrates and their variation within the bay.

Acknowledgements We would like to extend our gratitude to the Universidad Autónoma de Occidente (UAdeO) for supporting this study, and to the environmental engineer Jorge Antonio Sandoval Romero for his technical support in the analysis of nitrates.

Data availability All data generated or analyzed during this study are included in this published article.

Declarations

Conflict of interest The authors declare no competing interests.

References

Amanollahi, J., Kaboodvandpour, S., & Majidi, H. (2017). Evaluating the accuracy of ANN and LR models to estimate the water quality in Zarivar International Wetland. *Iran. Natural Hazards, 85*(3), 1511–1527. https://doi.org/10.1007/s11069-016-2641-1

Barrett, D. C., & Frazier, A. E. (2016). Automated Method for Monitoring Water Quality Using Landsat Imagery. *Water, 8*(6), 257. https://doi.org/10.3390/w8060257

Bruesewitz, D. A., Hoellein, T. J., Mooney, R. F., Gardner, W. S., & Buskey, E. J. (2017). Wastewater influences nitrogen dynamics in a coastal catchment during a prolonged drought. *Limnology and Oceanography, 62*(S1), S239–S257. https://doi.org/10.1002/lno.10576

Capone, D. G., & Hutchins, D. A. (2013). Microbial biogeochemistry of coastal upwelling regimes in a changing ocean. *Nature Geoscience, 6*(9), 711–717. https://doi.org/10.1038/ngeo1916

Chang, N. B., Imen, S., & Vannah, B. (2014). Remote sensing for monitoring surface water quality status and ecosystem state in relation to the nutrient cycle: A 40-year perspective. *Critical Reviews in Environmental Science and Technology, 45*(2), 101–166. https://doi.org/10.1080/10643389.2013.829981

Chen, Y. L. L., & Chen, H. Y. (2003). Nitrate-based new production and its relationship to primary production and chemical hydrography in spring and fall in the East China Sea. *Deep Sea Research Part II: Topical Studies in Oceanography, 50*(6), 1249–1264. https://doi.org/10.1016/S0967-0645(03)00021-3

Climate Computing project (CLICOM). (2016). *Datos climáticos diarios del CLICOM del SMN a través de su plataforma web del CICESE*. Retrieved July 15, 2016, from http://clicom-mex.cicese.mx

Comisión Nacional del Agua (CONAGUA). (2022). Calidad del agua (nacional). Subdirección General Técnica. Retrieved June 06, 2022, from http://sina.conagua.gob.mx/sina/tema.php?tema=calidadAgua&ver=mapa

Correll, D. L. (1998). The role of phosphorus in the eutrophication of receiving waters: A review. *Journal of Environment Quality, 27*(2), 261–266. https://doi.org/10.2134/jeq1998.00472425002700020004x

Diario Oficial de la Federación (DOF). (1989). *Criterios Ecológicos de Calidad del Agua CE- CCA-001/8*. http://www.dof.gob.mx/nota_to_imagen_fs.php?codnota=4837548&fecha=13/12/1989&cod_diario=208204

Dong, G., Hu, Z., Liu, X., Fu, Y., & Zhang, W. (2020). Spatio-Temporal Variation of Total Nitrogen and Ammonia Nitrogen in the Water Source of the Middle Route of the South-To-North Water Diversion Project. *Water, 12*(9), 2615. https://doi.org/10.3390/w12092615

Goes, J. I., Gomes, H. D. R., Saino, T., Wong, C. S., & Mordy, C.W. (2004). Exploiting MODIS data for estimating sea surface nitrate from space. *Eos*, 85(44). https://doi.org/10.1029/2004EO440001

Goes, J. I., Saino, T., Oaku, H., & Jiang, D. L. (1999). A method for estimating sea surface nitrate concentrations from remotely sensed SST and chlorophyll a-a case study for the north Pacific Ocean using OCTS/ADEOS data. *IEEE Transactions on Geoscience and Remote Sensing, 37*(3), 1633–1644. https://doi.org/10.1109/36.763279

González-Márquez, L. C., Figueroa-Moreno, M. A., Hansen-Rodríguez, I. R., Rodríguez-Gallegos, H. B., & Trigueros-Salmerón, Á. (2014). Fosfatos en agua de drenaje agrícola: cuenca baja del Río Sinaloa. *Ciencia Desde El Occidente*, 1(2).

González-Márquez, L. C., Torres-Bejarano, F. M., Torregroza-Espinosa, A. C., Hansen-Rodríguez, I. R., Rodríguez-Gallegos, H. B. (2018). Use of LANDSAT 8 images for depth and water quality assessment of El Guájaro reservoir, Colombia. *Journal of South American Earth Sciences*, *82*, 231–238. https://doi.org/10.1016/j.jsames.2018.01.004

Guo, H., Huang, J. J., Chen, B., Guo, X., & Singh, V. P. (2021). A machine learning-based strategy for estimating non-optically active water quality parameters using Sentinel-2 imagery. *International Journal of Remote Sensing*. https://doi.org/10.1080/01431161.2020.1846222

Haggard, B. E., Stanley, E. H., & Storm, D. E. (2005). Nutrient retention in a point-source-enriched stream. *Journal of the North American Benthological Society, 24*(1), 29–47. https://doi.org/10.1899/0887-3593(2005)024%3c0029:NRIAPS%3e2.0.CO;2

Hutchinson, G. E. (1973). Eutrophication: The scientific background of a contemporary practical problem. *American Scientist, 61*(3), 269–279.

Joo, H., Lee, D., Son, S. H., & Lee, S. H. (2018). Annual new production of phytoplankton estimated from MODIS-derived nitrate concentration in the East/Japan Sea. *Remote Sensing, 10*(5), 22–24. https://doi.org/10.3390/rs10050806

Khattab, M. F. O., & Merkel, B. J. (2013). Application of Landsat 5 and Landsat 7 images data for water quality mapping in Mosul Dam Lake, Northern Iraq. *Arabian Journal of Geosciences, 7*, 3557–3573. https://doi.org/10.1007/s12517-013-1026-y

Kloiber, S. M., Brezonik, P. L., Olmanson, L. G., & Bauer, M. E. (2002). A procedure for regional lake water clarity assessment using Landsat multispectral data. *Remote Sensing of Environment, 82*(1), 38–47. https://doi.org/10.1016/S0034-4257(02)00022-6

Kouadri, S., Pande, C. B., Panneerselvam, B., & Moharir, K. N. (2022a). Prediction of irrigation groundwater quality parameters using ANN, LSTM, and MLR models. *Environmental Science and Pollution Research International, 29*, 21067–21091. https://doi.org/10.1007/s11356-021-17084-3

Kouadri, S., Pande, C. B., Panneerselvam, B., Moharir, K. N., & Elbeltagi, A. (2022b). Prediction of irrigation groundwater quality parameters using ANN, LSTM, and MLR models. *Environmental Science and Pollution Research International, 29*(14), 21067–21091. https://doi.org/10.1007/s11356-021-17084-3

Lim, J., & Choi, M. (2015). Assessment of water quality based on Landsat 8 operational land imager associated with human activities in Korea. *Environmental Monitoring and Assessment, 187*(6), 1–17. https://doi.org/10.1007/s10661-015-4616-1

Lyle-Fritch, P. L. (2003). Laguna Playa Colorada-Santa María La Reforma. Ficha Informativa de los Humedales de Ramsar (FIR). Mazatlán, Sinaloa. Retrieved June 30, 2016, from https://rsis.ramsar.org/RISapp/files/RISrep/MX1340RIS.pdf

Martínez-López, A., Escobedo-Urías, D. C., Ulloa-Pérez, A. E., & Aguirre, R. (2008). Dynamics of a Prorocentrum minimum bloom along the northern coast of Sinaloa. *Mexico. Continental Shelf Research, 28*(14), 1693–1701. https://doi.org/10.1016/j.csr.2008.02.017

Masocha, M., Mungenge, C., & Nhiwatiwa, T. (2018). Remote sensing of nutrients in a subtropical African reservoir: Testing utility of Landsat 8. *Geocarto International, 33*(5), 458–469. https://doi.org/10.1080/10106049.2016.1265596

Mishra, A. P., Khali, H., Singh, S., Pande, C. B., Singh, R., & Chaurasia, S. K. (2021). An assessment of in-situ water quality parameters and its variation with Landsat 8 Level 1 surface reflectance datasets. *International Journal of Environmental Analytical Chemistry,* 1–23. https://doi.org/10.6084/m9.figshare.15073284.v1

Mishra, A. P., Singh, S., Jani, M., Singh, K. A., Pande, C. B., & Varade, A. M. (2022). Assessment of water quality index using analytic hierarchy process (AHP) and GIS: A case study of a struggling Asan River. *International Journal of Environmental Analytical Chemistry*, 1–13. https://doi.org/10.1080/03067319.2022.2032015

Mouw, C. B., Greb, S., Aurin, D., DiGiacomo, P. M., Lee, Z., Twardowski, M., Binding, C., Hu, C., Ma, R., Moore, T., Moses, W., & Craig, S. E. (2015). Aquatic color radiometry remote sensing of coastal and inland waters: Challenges and recommendations for future satellite missions. *Remote Sensing of Environment, 160*, 15–30. https://doi.org/10.1016/j.rse.2015.02.001

Paudel, B., Montagna, P. A., & Adams, L. (2019). The relationship between suspended solids and nutrients with variable hydrologic flow regimes. *Regional Studies in Marine Science, 29*, 100657. https://doi.org/10.1016/j.rsma.2019.100657

Ramsar. (2022). Laguna Playa Colorada-Santa María La Reforma. Ramsar Sites Information Service. Retrieved June 02, 2022, from https://rsis.ramsar.org/ris/1340

Ruiz-Fernández, A., & Páez-Osuna, F. (2004). Comparative survey of the influent and effluent water quality of shrimp ponds on Mexican farms. *Water Environment Research, 76*, 5–14. https://doi.org/10.2175/106143004X141528

Smith, V. H., Tilman, G. D., & Nekola, J.C. (1999). Eutrophication: impacts of excess nutrient inputs on freshwater, marine, and terrestrial ecosystems. *Environmental Pollution*, 100(1–3). https://doi.org/10.1016/S0269-7491(99)00091-3

Tappin, A. D., Millward, G. E., & Fitzsimons, M. F. (2010). Particle–water interactions of organic nitrogen in turbid estuaries. *Marine Chemistry, 122*(1–4), 28–38. https://doi.org/10.1016/j.marchem.2010.08.006

Topp, S. N., Pavelsky, T. M., Jensen, D., Simard, M., & Ross, M. R. V. (2020). Research trends in the use of remote sensing for inland water quality science: Moving towards multidisciplinary applications. *Water, 12*(1), 1–34. https://doi.org/10.3390/w12010169

Torbick, N., Hession, S., Hagen, S., Wiangwang, N., Becker, B., & Qi, J. (2013). Mapping inland lake water quality across the Lower Peninsula of Michigan using Landsat TM imagery. *International Journal of Remote Sensing, 34*(21), 7607–7624. https://doi.org/10.1080/01431161.2013.822602

Vermote, E., Justice, C., Claverie, M., & Franch, B. (2016). Preliminary analysis of the performance of the Landsat 8/OLI land surface reflectance product. *Remote Sensing of Environment*, 185, 46–56. https://doi.org/10.1016/j.rse.2016.04.008

Wang, D., Cui, Q., Gong, F., Wang, L., He, X., & Bai, Y. (2018). Satellite retrieval of surface water nutrients in the coastal regions of the East China Sea. *Remote Sensing*, 10(12). https://doi.org/10.3390/rs10121896

Wang, D., Xie, X., Tang, W., Pan, H., & Luo, J. (2021). Suitability of Nansha mangrove wetland for high nitrogen shrimp pond wastewater treatment. *Bulletin of Environment Contamination and Toxicology, 106*(2), 349–354. https://doi.org/10.1007/s00128-020-03060-z

Wang, X., & Yang, W. (2019). Water quality monitoring and evaluation using remote sensing techniques in China: A systematic review. *Ecosystem Health and Sustainability, 5*(1), 47–56. https://doi.org/10.1080/20964129.2019.1571443

Wu, C., Wu, J., Qi, J., Zhang, L., Huang, H., Lou, L., & Chen, Y. (2010). Empirical estimation of total phosphorus concentration in the mainstream of the Qiantang River in China using Landsat TM data. *International Journal of Remote Sensing, 31*(9), 2309–2324. https://doi.org/10.1080/01431160902973873